ЖЭТФ, 2014, том 145, вып. 2, стр. 218–222 © 2014

GENERATION AND CHARACTERIZATION OF Nd–Fe–B–C NANOPARTICLES BY PULSED Nd:YAG LASER ABLATION IN LIQUID

H. R. Dehghanpour *

Physics Department, Tafresh University, Tafresh, Iran

Received July 27, 2013

We have generated Nd–Fe–B–C nanoparticles by Nd:YAG (1064 nm) laser irradiation in distilled water. Exposure times were 1, 5, and 10 min. Characterization of such nanoparticles in terms of their size distribution, shape, and chemical composition was carried out by transmission electron microscopy, energy-dispersive X-ray, and Fourier transform infrared spectroscopy. To investigate the nanoparticle stability, the size distribution of nanoparticles was measured two weeks after the nanoparticle generation, using dynamic light scattering. Investigations with the help of the atomic force microscope and magnetic force microscope showed other aspects of the generated nanoparticles.

DOI: 10.7868/S0044451014020035

1. INTRODUCTION

Research in the area of magnetism and magnetic materials is a rich combination of synthesis, characterization, theoretical concepts, and engineering applications [1]. Hard magnetic materials are used in hard disk drivers, motors, generators, loudspeakers, magnetic sensors, etc. Nd–Fe–B–C magnets are well known because of their strong, permanent magnetic properties, high coercitivity, and high magnetic remanence. Magnetic nanoparticles are used in ferrofluids [2], refrigeration systems [3], and multiterabit information storage devices [4, 5]. In the last decades, intensive efforts have been invested into the development of new methods for generation of nanoparticles. In particular, magnetic nanoparticles have attracted great attention because of their widespread application prospects in biomedicine and information technology [6–9]. Laser ablation in liquids offers an approach to the fabrication of pure nanoparticle colloids of various materials. Until now, mainly metal and ceramic colloids have been generated using this method, including several studies on laser-generated magnetic nanoparticles [10–12]. There are a few reports concerning laser-based generation of colloidal magnetic alloys [13, 14]. Here, Nd–Fe–B–C nanoparticles are generated in distilled water using Q-switched Nd:YAG laser (1064 nm). Geometrical and chemical properties of those nanoparticles are then revealed. This could be attractive for microtechnology applications such as the development of micromotors or magnetic micropumps [15, 16].

2. EXPERIMENTAL SECTION

2.1. Synthesis methods

Figure 1 shows a schematic diagram of the experimental setup. An Nd–Fe–B–C magnet target was immersed in distilled water and fixed on a plate connected to the motor rotating the target (5 rev/min) to prevent deep laser crater creation. Nanoparticles were fabricated by pulsed nanosecond laser irradiation using Nd:YAG laser at 1064 nm. The laser shots are characterized by the 10 ns duration, 5 Hz repetition rate, 60 mJ pulsed energy, and 6 J/cm^2 energy density. The laser beam was focused directly on a target 2 mm in thickness. It was situated at the bottom of a glass beaker filled with 10 ml of distilled water, corresponding to 6 mm of liquid height above the target at room temperature using a lens with a 10 cm focal point. The focusing area, power, and energy density of the laser were properly controlled by the relative displacement of the target and the lens. The exposure times were 1, 5, and 10 min. After laser irradiation, drops of liquid containing nanoparticles were sprayed on a plate

*E-mail: h.dehghanpour@aut.ac.ir

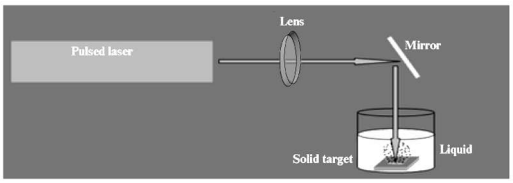

Fig. 1. Experimental setup for fabricating Nd–Fe–B–C nanoparticles in distilled water by laser irradiation

of glass. Then, after water evaporation remained, the materials were collected.

2.2. Characterization methods

Geometrical aspects of the nanoparticles were studied by transmission electron microscopy (TEM), Philips model EM 208 S. Chemical composition of the bulk and the nanoparticles was investigated using energy-dispersive X-rays (EDX). The time effect on the nanoparticle sizes was investigated by dynamic light scattering (DLS) two weeks after the nanoparticle generation.

3. RESULTS AND DISCUSSIONS

The TEM can yield information such as the particle size, size distribution, and morphology of the nanoparticles. In particle size measurement, microscopy is the only method in which individual particles are directly observed and measured [17]. Typically, the calculated sizes are expressed as the diameter of a sphere that has the same projected area as the projected image of the particle. Manual or automatic techniques are used for particle size analysis. The manual technique is usually based on the use of a marking device moved along the particle to obtain linear dimensional measures of the particles, which are then added and divided by the number of particles to obtain a mean result [18]. In combination with diffraction studies, microscopy becomes a very valuable aid to characterization of nanoparticles [19]. TEM micrographs of the Nd–Fe–B–C nanoparticles fabricated by a Q-switched Nd:YAG laser and various exposure times (1, 5, and 10 min) as well as the corresponding size distributions are shown in Fig. 2.

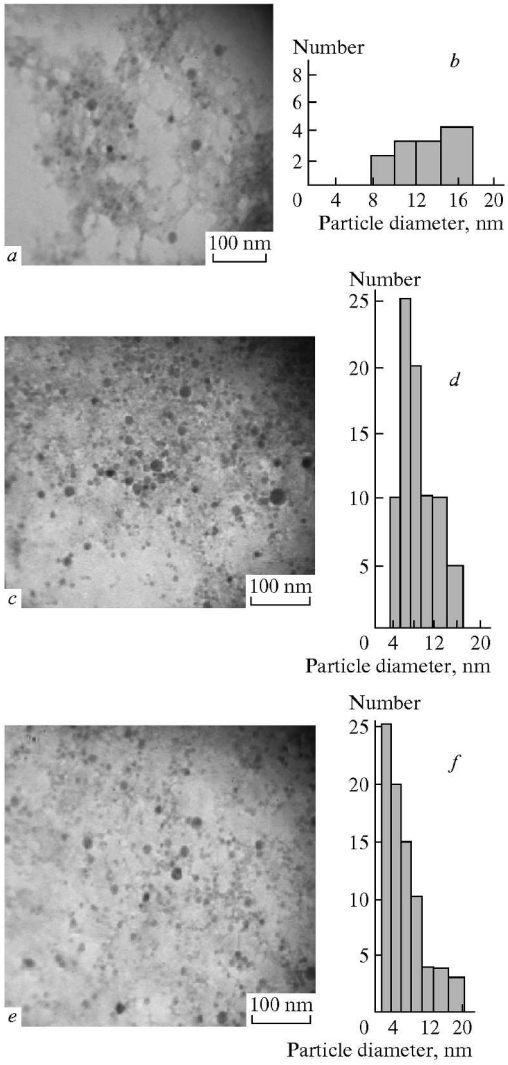

Fig. 2. TEM images of nanoparticles fabricated by the Nd:YAG laser with (a) 1 min, (c) 5 min, and (e) 10 min exposure times; b, d, and f are the corresponding size distributions

After the laser is switched off, the fragmentation process ceases and the aggregation process proceeds. A TEM image shows the presence of nearly spherical particles. In view of the process of formation of nanoparticles and rapid quenching of the ablated material into the liquid, this is their most probable morphology [20]. The average size of the nanoparticles generated by pulsed Nd:YAG laser radiation for 1, 5, and

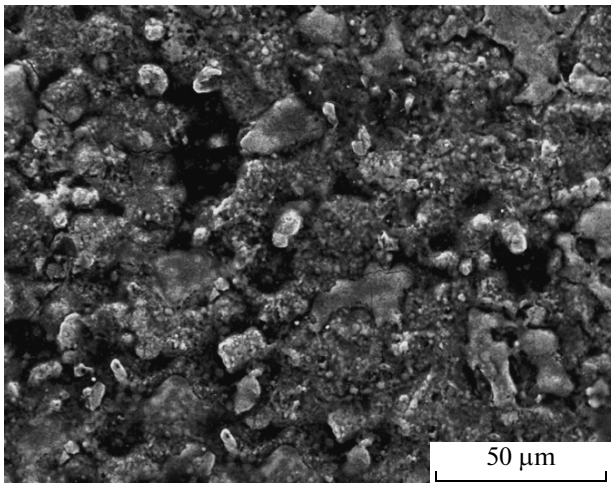

Fig. 3. SEM of the target surface after a 10 min laser exposure

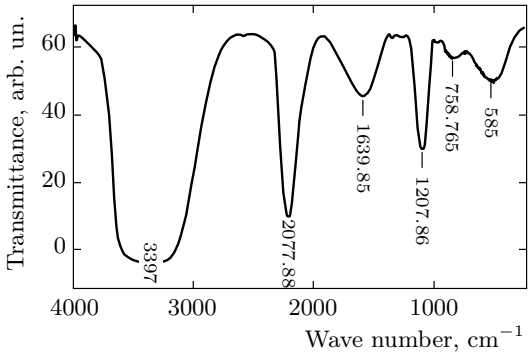

Fig. 4. Transmittance spectrum of the suspension solution of nanoparticles

10 min exposure times are 13.7, 8.35, and 6.23 nm respectively.

It is worth noting that the largest particles most likely result from the aggregation of smaller particles. Their number is relatively small and does not influence the size distribution significantly. Such aggregation is known and dicussed in [20]. It can be explained by the tendency of lowering a colloidal system energy to achieve a more stable state. The mean diameter and the size distribution of the nanoparticles decrease as the ablation time increases. This can be explained by a redistribution of the size of the particles through their interaction with the laser beam. On the other hand, creation of nanoparticles near the target reduces the laser–target interaction and is effective on the number and size of the nanoparticles [21].

Figure 3 shows a scanning electron microscopy (SEM) image of the target surface after a 10 min laser exposure on it. There is a mixture of melting and ablating process on the target surface due to laser irradiation. The nanoparticle generation may be caused by ablation and by the superheated surface above its critical thermal point.

Table. Transmittance wave numbers and the corresponding bonds

Wave number, cm^{-1}	Bond
585	Fe–O
758.75	Fe–O–H
1207.86	B–O–B
1639.85	C=O
2077.88	Nd–Fe–C

The Fourier transform infrared spectroscopy (FTIR) is a very sensitive and one of the most used spectroscopy methods applied in characterizing the material structure. Figure 4 shows an FTIR transmittance spectrum of the suspension solution of the nanoparticles. Despite the 3397 cm^{-1} peak corresponding to the OH band of water, we see a set of peaks, whose corresponding bonds [22, 23] are collected in the Table. In the nanoparticles constructive elements of the target (except Nd) had a strong oxidation due to the aqueous environment.

Figure 5 shows the results of (EDX) microanalyses of the fabricated nanoparticles. As the figure shows, constructive elements of the target (Nd, F, B, and C) construct the nanoparticles. The existence of silicon in the nanoparticles may be due to the ablated silicon from the glass container or the plate of glass on which the drops containing nanoparticles were speared for harvesting the nanoparticles.

As a result, the chemical composition of the target and nanoparticles is the same. Although TEM is the experimental technique most extensively used for obtaining general information on particle morphology and evaluating the size distribution, the atomic force microscope (AFM) method has been established as a complementary and very useful method for characterization of shapes in nanoworld. In order to investigate nanoparticle stability, two weeks after the nanoparticle generation, their size distribution was measured using AFM and DLS. Figure 6 shows AFM images of nanoparticles (10 min laser exposure) two weeks after the nanoparticle fabrication. The particle size is between 15 and 70 nm with the average near 30 nm.

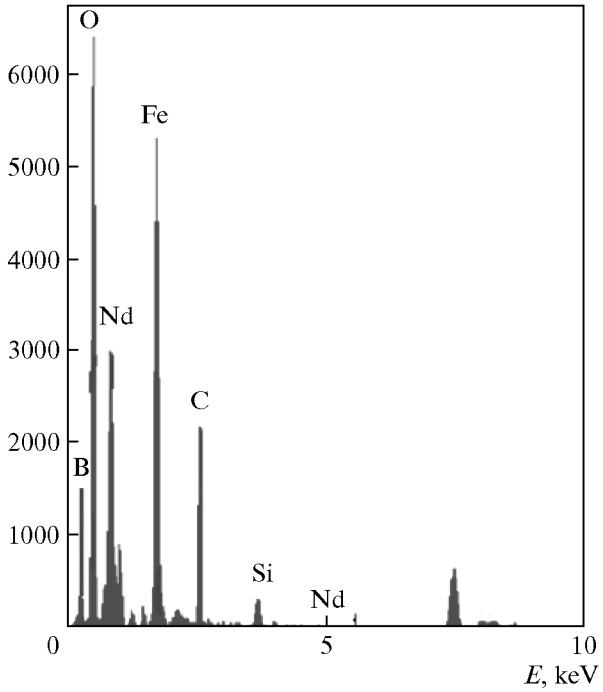

Fig. 5. EDX microanalyses of the fabricated nanoparticles

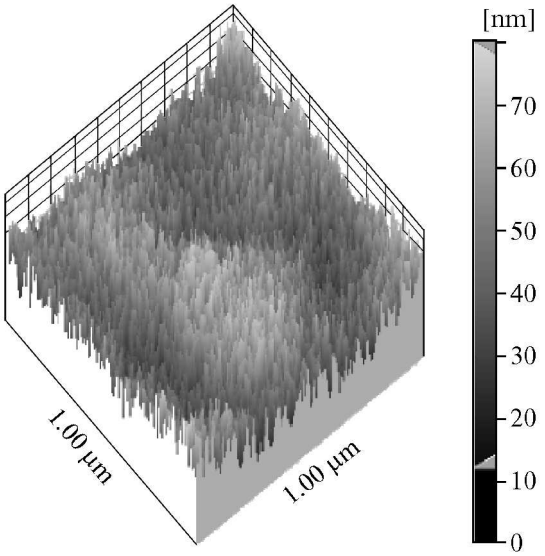

Fig. 6. AFM image of Nd–Fe–B–C nanoparticles fabricated by a Q-switched Nd:YAG laser in distilled water

Size distributions of the nanoparticles based on the results of DLS for a sample with 10 min exposure time are shown in terms of number, volume, and light intensity in Fig. 7. The size distribution versus numbers (Fig. 7*a*) verified the size distribution obtained by AFM. On the other hand, the size distribution versus

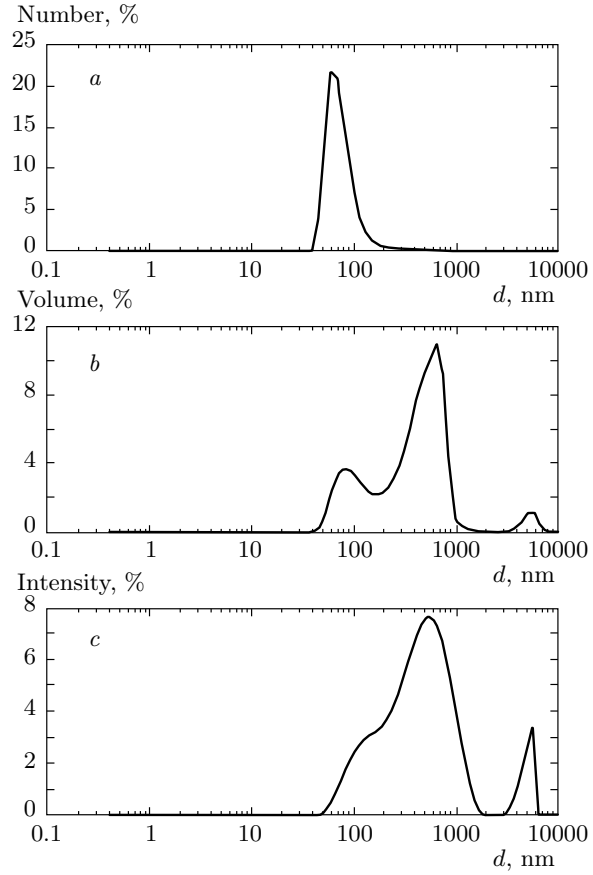

Fig. 7. After two weeks, size distribution versus (*a*) the number of nanoparticles, (*b*) volume of the nanoparticles, and (*c*) scattered light intensity by nanoparticles, fabricated by a 10 min Nd:YAG laser exposure using DLS

volume and intensity (Figs. 7*b* and 7*c*) shows the presence of particles with larger sizes but lower in numbers. Figure 8 depicts magnetic domains of nanoparticles obtained using a magnetic force microscope (MFM).

4. CONCLUSION

In this work, we have examined the method of laser nanoparticle generation in liquid for fabrication of hard magnetic alloy nanoparticles. Microstructural investigation, magnetic properties, and chemical composition of the nanoparticles were performed by FTIR, EDX, TEM, DLS, AFM, and MFM. The resulting chemical composition of the nanoparticles depends on the elemental composition of the target. In the nanoparticles, constructive elements of the target (except Nd) had a strong oxidation due to the aqueous environment. The magnetic property of the nanoparticles was detectable, and they had considerable magnetic field. It is worth

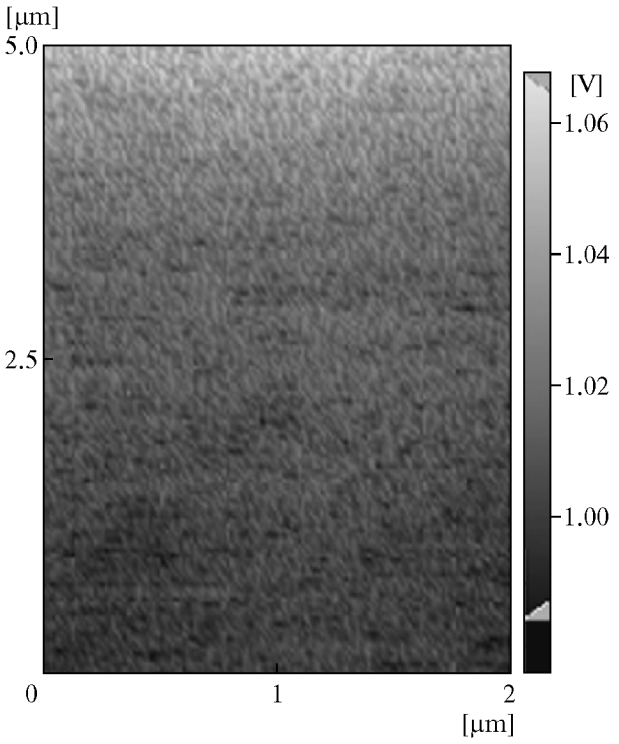

Fig. 8. MFM image of nanoparticles fabricated by a Q-switched Nd:YAG laser in distilled water

noting that investigation of changing the laser dose, wavelength, and exposure time plays an important role in completing this work.

REFERENCES

1. J. M. D. Coey, J. Magn. Magn. Mater. **226–230**, 2107 (2001).
2. Y. Sahoo, A. Goodarzi, M. T. Swihart et al., J. Phys. Chem. B **109**, 3879 (2005).
3. R. D. Shull, IEEE Trans. Magn. **29**, 2614 (1993).
4. X. Sun, Y. Huang, and D. E. Nikles, Int. J. Nanotechnol. **1**, 328 (2004).
5. T. Hyeon, Chem. Comm. **8**, 927 (2003).
6. S. Jiguet, M. Judelewicz, S. Mischler et al., Microelectron. Eng. **83**, 1273 (2006).
7. S. Peterson, J. Jakobi, and S. Barcikowski, Appl. Surf. Sci. **255**, 5435 (2009).
8. S. Peterson and S. Barcikowski, Adv. Func. Mater. **19**, 1 (2009).
9. K. Nakata, Y. Hu, O. Uzun et al., Adv. Mater. **1**, 9999 (2008).
10. T. Tsuji, T. Hamagami, T. Kawamura et al., Appl. Surf. Sci. **243**, 214 (2005).
11. A. V. Kabashin, M. Meunier, C. Kingston, and J. H. T. Luong, J. Phys. Chem. B **107**, 4527 (2003).
12. P. V. Kazakevich, V. V. Voronov, A. V. Simakin, and G. A. Shafeev, Quant. Electr. **34**, 951 (2004).
13. J. Jakobi, S. Peterson, A. M. Manjon et al., Langmuir Lett. **26**, 6892 (2010).
14. H. R. Dehghanpour, J. Russ. Laser. Res. **33**, 431 (2012).
15. M. Feldmann, S. Demming, and S. Buttgenbach, Proc. Nanotech. **3**, ISBN 1-4200-6184-4 (2007).
16. A. Waldschik, M. Feldmann, and S. Buttgenbach, in *Proc. Actuator* (2008), p. 669.
17. T. Allen, *Particle Size Measurement*, Chapman and Hall (1997).
18. A. Jilavenkatesa, S. J. Dapkunas, and H. L. Lin-Sien, *Particle Size Characterization*, NIST Recommended Practical Guide (2001).
19. C. H. Liang, A. W. Colightly, and J. R. Castleman, J. Phys. Chem. B **110**, 19979 (2006).
20. X. P. Zhu, T. Suzuki, T. Nakayama et al., Chem. Phys. Lett. **427**, 127 (2006).
21. R. Mahfouz, F. J. C. S. Aires, A. Brenier et al., Appl. Surf. Sci. **254**, 5181 (2008).
22. M. Toders, S. Filip, and I. Ardelean, J. Optoelectron. Adv. Mat. **8**, 1121 (2006).
23. E. I. Kamitsos, M. A. Karakassides, and G. D. Chryssikos, J. Phys. Chem. **91**, 1073 (1987).